

## Acknowledgements

We wish to thank the M.I.T. Center for Materials Science and Engineering (NSF-MRL Core Fund DMR 78-24185) for partial support of this work. M.E.G. is grateful for graduate student support from Polaroid Corporation.

## References

- 1 MacDiarmid, A. G. and Heeger, A. J. *Synth. Metals* 1979/80, **1**, 101
- 2 MacInnes, Jr., D., Druy, M. A., Nigrey, P. J., Nairns, D. P., MacDiarmid, A. G. and Heeger, A. J. *Chem. Comm.* 1981, **317**
- 3 Shacklette, L. W., Chance, R. R., Ivory, D. M., Miller, G. G. and Baughman, R. H. *Synth. Metals* 1979/80, **1**, 307
- 4 Chance, R. R., Shacklette, L. W., Miller, G. G., Ivory, D. M., Sowa, J. M., Elsenbaumer, R. L. and Baughman, R. H. *Chem. Comm.* 1980, **348**; Rabolt, J. F., Clarke, T. C., Kanazawa, K. K., Reynolds, J. R. and Street, G. B. *ibid* 1980, **347**
- 5 Kanazawa, K. K., Diaz, A. F., Geiss, R. H., Gill, W. D., Kwak, J. F., Logan, J. A., Rabolt, J. F. and Street, G. B. *ibid* 1979, **854**
- 6 Wnek, G. E., Chien, J. C. W., Karasz, F. E. and Lillya, C. P. *Polymer* 1979, **20**, 1441
- 7 Gibson, H. W., Bailey, F. C., Epstein, A. J., Rommelmann, H. and Pochan, J. M. *Chem. Comm.* 1980, **426**
- 8 Chien, J. C. W., Wnek, G. E., Karasz, F. E. and Hirsch, J. A. *Macromolecules* 1981, **14**, 479
- 9 Enkelman, V., Muller, H. and Wegner, G. *Synth. Metals* 1979/80, **1**, 185
- 10 Kletter, M. J., Woerner, T., Pron, A., MacDiarmid, A. G., Heeger, A. J. and Park, Y. W. *Chem. Comm.* 1980, **426**
- 11 Ito, T., Shirakawa, H. and Ikeda, S. *J. Polym. Sci., Polym. Chem. Edn.* 1974, **12**, 11
- 12 Shirakawa, H., Ito, T. and Ikeda, S. *Polym. J.* 1973, **4** 460

## Accuracy of fluorescence polarization measurements and discrimination of uniaxial deformation models

Manfred Hennecke and Jürgen Fuhrmann

Fachbereich Chemie, Universität Kaiserslautern, Postfach 3069, D-6750 Kaiserslautern, FRG

(Received 4 January 1982)

The technique of fluorescence polarization is examined for the influence of measuring errors on the light intensities and the depolarization correction parameter  $p$ . It is shown how the accuracy of the received orientation coefficients depends on the measured quantities, especially on the absolute value of  $p$ , the latter restricting the polymer systems to which the method is suitable. The lowest accuracy needed to take advantage of the information on the fourth moment of the orientation distribution function is calculated as well as the considerable accuracy required to discriminate orientation models, e.g. the pseudoaffine model, from others.

**Keywords** Fluorescence polarization; deformation models; orientation distribution function; experimental accuracy requirement

## Introduction

With the fluorescence polarization method (fpm), the 2nd and 4th moment of the orientational distribution function (odf) of the anisotropic chromophores are determined<sup>1,2</sup>. In the case of uniaxial symmetry of both the rigid anisotropic matrix (e.g. polymer films or fibres) and the fluorescent molecule, the angle  $\theta$ , i.e. the angle between the orientation axis of the sample and the molecular orientation axis of the fluorescent molecule, is the only variable in the odf. In this case, with the fpm the moments  $\langle \cos^2\theta \rangle$  and  $\langle \cos^4\theta \rangle$  are obtained. Equivalent to the presentation of moments is the use of the 2nd and the 4th coefficient of the development of the odf in a series of Legendre polynomials. These two coefficients usually allow for an approximate graph of the odf<sup>3</sup>.

In the aforementioned case of symmetry three polarized fluorescence components, e.g.  $I_{ZZ}$ ,  $I_{ZY}$ , and  $I_{YY}$  ( $Z$  orientation axis of the sample,  $X$  optical beam axis of the apparatus; first subscript denotes the polarizer direction, second subscript the analyser direction) are independent<sup>1</sup>. These three light intensities must be measured. Additionally, the photophysical parameter  $p_m$  which indicates the optical anisotropy of the absorption tensor  $a = (a_{ij})$  and the emission tensor  $e = (e_{ij})$  must be known to determine  $\langle \cos^2\theta \rangle$  and  $\langle \cos^4\theta \rangle$ . There is only one

parameter  $p_m$  under the condition of rotationellipsoidic anisotropy of absorption and emission transition moments relative to the uniaxial symmetry of the fluorescent molecule mentioned above.

$$p_m = \frac{2a_{22}}{2a_{22} + a_{33}} = \frac{2e_{22}}{2e_{22} + e_{33}} \quad (1)$$

The parameter  $p_m$  ( $0 \leq p_m \leq 2/3$  for  $a_{22} \leq a_{33}$ ; if  $a_{22} > a_{33}$  the true  $p_m$  may be calculated by exchanging  $a_{22}$  and  $a_{33}$ ) may be measured independently by means of a sample of known orientation, usually an isotropic sample.  $p_m$  is related to the fundamental fluorescence anisotropy  $r_0$  by

$$p_m = 2/3 - 1/3\sqrt{10r_0} \quad (2)$$

where

$$r_0 = \left( \frac{I_{ZZ} - I_{ZY}}{I_{ZZ} + 2I_{ZY}} \right)_{\text{isotropic}} \quad (3)$$

is measured with two polarized intensities in the isotropic state.

In a real sample the so-measured parameter  $p_m$  (and respective  $r_0$ ) refers not only to the intramolecular properties but additionally may correct depolarization of fluorescence due to scattering, e.g. at the surface or at crystallites. For separation from the molecular constant  $p_m$ , the measured parameter is named  $p$  in this note with  $p > p_m$  in a non-ideal and  $p = p_m$  in an optically ideal sample. Assuming that the depolarization is independent of both the anisotropy of the sample and the wavelength of the exciting and the fluorescent light, no further correction is necessary. Otherwise, up to four scattering correction coefficients must be measured at each degree of deformation<sup>4</sup>, an apparatus requirement which has not yet been realized for measurements during stretching.

To take advantage of the 4th moment information on the type of the odf, the precision of the experimental results must be high. This is generally believed to be so since the moments are not independent from one another, especially if presumptions on the shape of the odf are made<sup>5</sup>. Furthermore, the truncation of the series limits the evaluation of the odf<sup>3,6</sup>. Unavoidably, the odf of the fluorescent moieties (labels, probe molecules, or intrinsic fluorescence of the matrix sample) must be correlated to the odf of the sample's structural units, in which one is usually interested.

*Influence of measurement errors on the orientation parameters*

The influence of an error in  $p$  and of a measurement error in the intensities\* on the values of  $\langle \cos^2\theta \rangle$ ,  $\langle \cos^4\theta \rangle$  was calculated numerically for different cases. First, the error is assumed to originate separately in each of the light intensities  $I_{ZZ}$ ,  $I_{ZY}$ ,  $I_{YY}$  and the parameter  $p$ . Secondly, the error is allowed to occur in all components (statistical noise), and in  $p$  (constant error due to the distinct determination) simultaneously. The percentage of error for  $p$  was calculated from  $r_0$  without exceeding the physical limits of  $p$ .

These calculations were performed with a microcomputer, normalizing  $K$  to 1. The constant  $K$  is the total fluorescence intensity of the sample<sup>7</sup>

$$K = \sum_{i,j} I_{i,j} \approx k \bar{e} d c Q \quad (i,j = X, Y, Z) \quad (4)$$

$$K = \frac{1}{3 - 2p + p^2} [(3 - 2p) I_{ZZ} + 8 I_{YY} + 4(3 - p) I_{ZY}] \quad (5)$$

containing the optical density  $\bar{e} d c$ , the quantum yield  $Q$ , and an instrumental constant  $k$ . Using the pseudoaffine deformation scheme (pad)<sup>8,9</sup> the change of the normalizing factor for  $K$  during stretching depends simply on the square root of the stretching ratio  $\lambda$  which refers to the change of thickness. The orientational coefficients of the pad are given by:

$$\langle \cos^2\theta \rangle = \frac{\lambda^3}{\lambda^3 - 1} \left( 1 - \frac{\arctan \sqrt{\lambda^3 - 1}}{\sqrt{\lambda^3 - 1}} \right) \text{ for } \lambda > 1 \quad (6)$$

$$\langle \cos^2\theta \rangle = \frac{\lambda^3}{1 - \lambda^3} \left( \frac{1}{2\sqrt{1 - \lambda^3}} \ln \frac{1 + \sqrt{1 - \lambda^3}}{1 - \sqrt{1 - \lambda^3}} - 1 \right) \text{ for } \lambda < 1 \quad (7)$$

\* Similar calculations were made with intensity ratios and can be obtained on request.

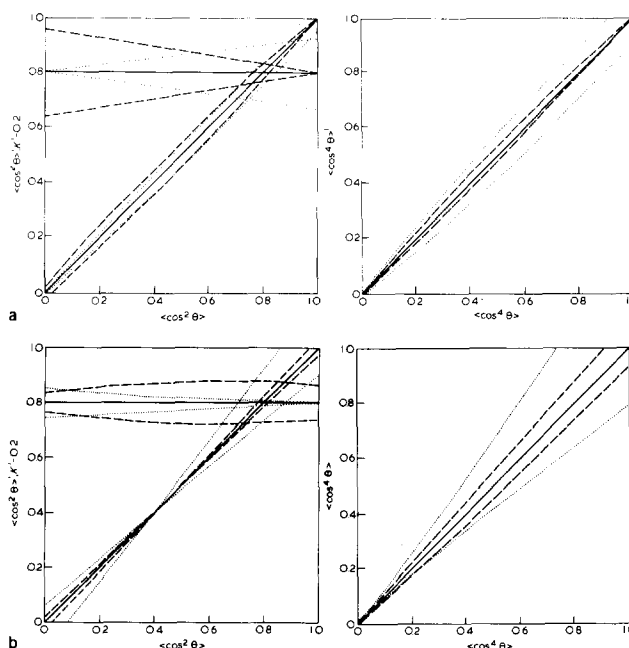


Figure 1 (a) Dotted curves ±20% error in  $I_{ZZ}$ ; broken curves ±20% error in  $I_{YY}$ . (b) Dotted curves ±50% error in  $p$ ; broken curves ±20% error in  $I_{ZY}$ . Error ranges of  $\langle \cos^2\theta \rangle'$  and  $K' - 0.2$  (left diagrams) drawn and  $\langle \cos^4\theta \rangle'$  (right diagrams) versus  $\langle \cos^2\theta \rangle$  and  $\langle \cos^4\theta \rangle$  respectively, calculated for the pad with a constant error (+ and -) in the quantity referred to and true values for the other quantities

$$\langle \cos^m\theta \rangle = \frac{\lambda^3}{(m-2)(\lambda^3-1)} ((m-1)\langle \cos^{m-2}\theta \rangle - 1) \quad m=4, 6, 8 \dots \quad (8)$$

If one assumes a relatively large error (for clarity of graphical presentation) of +20% and -20% in the intensities and +50% and -50% in  $p$ , and a typical absolute value of  $p=0.2$ , the curves of Figure 1 can be calculated. In these curves  $\langle \cos^2\theta \rangle'$ ,  $K' - 0.2$ , and  $\langle \cos^4\theta \rangle'$  are the erroneous values calculated with the +20% and the -20% error of the indicated fluorescence intensity, resp. the +50% and -50% error in  $p$ . They are plotted versus the true values of  $\langle \cos^2\theta \rangle$  and respective  $\langle \cos^4\theta \rangle$  values. The curves show the very different role of the individual components in the orientational results, especially as a function of mean orientation. If one is interested in  $\langle \cos^4\theta \rangle$  or higher oriented samples,  $I_{ZZ}$ ,  $I_{ZY}$ , and  $p$  must be measured with greater accuracy. For the determination of  $\langle \cos^2\theta \rangle$  in the medium range,  $I_{ZZ}$  and  $I_{YY}$  are more important than  $I_{ZY}$  or  $p$ . It should be realized, however, that these results depend on the absolute value of  $p$  which thus may influence the experimental procedure, e.g. the measuring times for the fluorescent components.

If one allows for statistical noise ( $\sigma=0.1$ ) in all three components and a constant error in  $p$  (+10%), which may be a realistic view, the total error in  $\langle \cos^2\theta \rangle$ ,  $\langle \cos^4\theta \rangle$ , and  $K$  is partially compensated. In this case the dependence of the relative error on the mean orientation is relatively weak in the region of  $0.2 < \langle \cos^2\theta \rangle < 1$  but depends strongly on the absolute value of the parameter  $p$ , as can be seen from the example in Figure 2. Herein, the average relative error of  $\langle \cos^2\theta \rangle$  and  $\langle \cos^4\theta \rangle$  (broken line) in the region  $0.5 < \langle \cos^2\theta \rangle < 1$  is plotted versus the absolute

value of  $p$ . It can be clearly seen that the accuracy declines dramatically on increasing  $p$ , especially in the case of  $\langle \cos^4\theta \rangle$  which shows an even higher percentage error. Similar curves are obtained by choosing different sets of error limits in the intensities and  $p$ .

This result demands a very high accuracy in measurement, as much as in the case of scatter-depolarizing samples, (e.g. partially crystallized polymers<sup>10</sup>, liquid crystalline polymers) as in the case of using chromophores showing an unfavourable value of  $p$  (e.g. the intrinsic fluorescence of some polymers<sup>11</sup>).

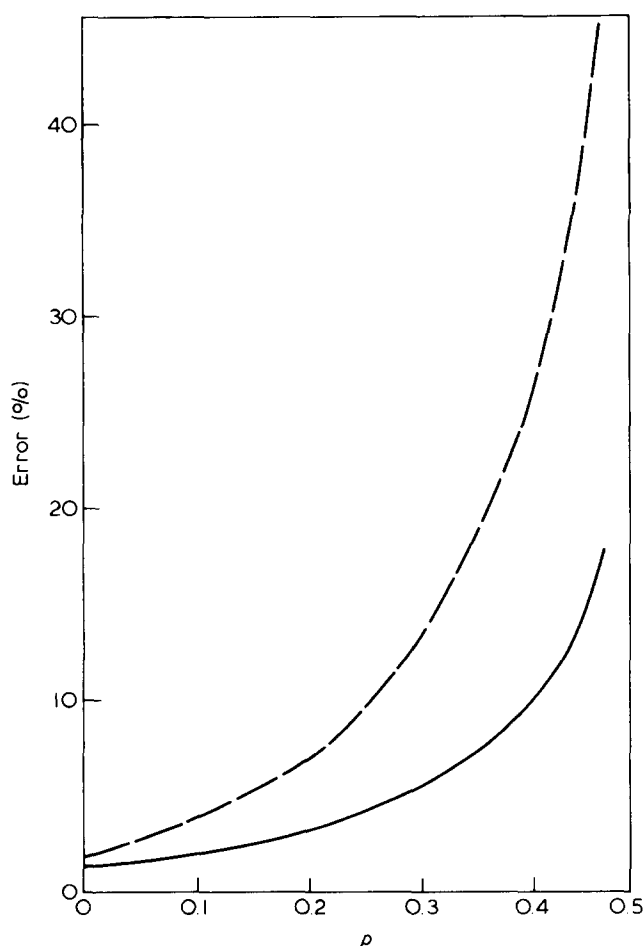


Figure 2 Dependence of the error in  $\langle \cos^2\theta \rangle$  (solid curve) and  $\langle \cos^4\theta \rangle$  (broken curve) on the absolute value of the correction parameter  $p$  (constant statistical noise of the intensities). Averaged in the region  $0.5 \leq \langle \cos^2\theta \rangle \leq 1$

Measurement accuracy required to distinguish between different types of odf

The claimed advantage of the fpm can only be utilized, if the accuracy of the 4th moment is sufficient. For example, let us consider the difference between the pad and a model which consists of a random odf (weight factor  $1 - \gamma$ ) and a superimposed completely oriented portion  $\gamma$  ( $0 \leq \gamma \leq 1$ ). For this simple model holds<sup>5</sup>

$$f_{(2)} = f_{(4)} = \gamma \tag{9}$$

and respectively

$$\begin{aligned} \langle \cos^4\theta \rangle &= 1.2 \langle \cos^2\theta \rangle - 0.2 \text{ for } \langle \cos^2\theta \rangle \geq 1/3 \\ \text{and} \\ \langle \cos^4\theta \rangle &= 0.6 \langle \cos^2\theta \rangle \text{ for } \langle \cos^2\theta \rangle \leq 1/3. \end{aligned}$$

The  $\langle \cos^4\theta \rangle$  values of both models differ most greatly at a value of  $\langle \cos^2\theta \rangle = 0.65$ ; the corresponding difference in the  $\langle \cos^4\theta \rangle$  values amounts to 0.052, i.e. 9% referred to the pad. On account of a clear distinction between the two models we have to limit the mean relative error to half the size of the difference at least. This condition applied, one gets the required accuracies in Table 1, which differ in the selected regions of  $\langle \cos^2\theta \rangle$ . The calculated accuracies already allow for partial compensation of the error in the three light intensities, which is reasonable in the case of Poisson-distributed photon counting error.

One may recognize from the third row of Table 1, that with usual conditions ( $p \approx 0.2$ ) an accuracy of better than 5% in each of the four measured quantities is just sufficient to discriminate the two models mentioned above. This accuracy may be obtained, from our experience, under favourable conditions, i.e. sufficiently high  $K$  value, for the light intensities but rarely for the correction parameter  $p$  with its inherent assumptions (see Introduction). Thus, limited evidence can be given to a certain orientation model from fpm results, without regard to the uncertainty arising from the series truncation. However, orientation models leading to values of  $\langle \cos^4\theta \rangle$  outside the accuracy range can be safely excluded. The calculation of  $\langle \cos^4\theta \rangle$  values is of no value, if their relative error comes up to the range governed by the inequalities<sup>5</sup>

$$\langle \cos^4\theta \rangle \geq (\langle \cos^2\theta \rangle)^2 \tag{10}$$

$$\text{and } \langle \cos^4\theta \rangle \leq \langle \cos^2\theta \rangle \tag{11}$$

Table 1 Difference between the pad and the superposition model (equation (9)) and the required measuring accuracy. For further explanation see text

Region of $\langle \cos^2\theta \rangle$	0-0.2	0.2-0.4	0.4-0.6	0.6-0.8	0.8-1
Averaged difference in $\langle \cos^4\theta \rangle$ in %	+43	+8.8	+10	+8.1	+3.3
Required accuracy in % of the light intensities and $r_0$ at $r_0 = 0.2$ ( $p = 0.19$ )	5.7	5.0	6.4	5.4	2.4
At $r_0 = 0.4$ ( $p = 0$ )	28.3	7.2	9.8	11.9	9.2

Table 2 Limiting measurement accuracy (in %) corresponding to the mathematically obtained limits (see equations (10) and (11)). For further explanation see text

Region of $\langle \cos^2\theta \rangle$	0-0.2	0.2-0.4	0.4-0.6	0.6-0.8	0.8-1
Averaged range of $\langle \cos^4\theta \rangle$ in %	82.7	54.5	33.8	18.2	6.2
Required accuracy in % of the light intensities and $r_0$ at $r_0 = 0.2$ ( $p = 0.19$ )	27	54	45	24	9.8
At $r_0 = 0.4$ ( $p = 0$ )	109	86	69	57	48

which determine an upper and lower limit for  $\langle \cos^4\theta \rangle$ . If one refers to the middle of the allowed  $\langle \cos^4\theta \rangle$  range, one obtains, according to the same concept as in Table 1, the results shown in Table 2. The data in Table 2 shows the experimental accuracy limit, i.e. error bars given in %, resulting from the mathematically well defined limits, e.g.  $\langle \cos^4\theta \rangle = 0.375 \pm 0.125$  at  $\langle \cos^2\theta \rangle = 0.5$ .

It follows from the data in Table 2, that even in the case of moderate accuracy, e.g. 10%, considerable reductions of the allowed range of  $\langle \cos^4\theta \rangle$  can be received. In such a way the type of the odf may be limited, allowing for discrimination between deformation models, provided they are sufficiently different.

### Conclusions

The fpm is an efficient and valuable tool in discriminating types of odf and types of deformation schemes if one selects photophysically ideal chromophores ( $p_m \rightarrow 0$ ) and if one investigates samples showing only moderate scattering depolarization. It is necessary to calculate and realize experimentally the required accuracy

in the light intensity measurements and in the determination of the correction parameter  $p$ , provided that the involved symmetry conditions of the sample and of the chromophore hold.

### References

- 1 Nobbs, J. H., Bower, D. I., Ward, I. M. and Patterson, D. *Polymer* 1974, **15**, 287
- 2 Jarry, J. P. and Monnerie, L. *J. Polym. Sci., A-2* 1978, **16**, 443
- 3 Bower, D. I. *J. Polym. Sci., Polym. Phys. Edn.* 1981, **19**, 93
- 4 Pinaud, F., Jarry, J. P., Sergot, P. and Monnerie, L. *Polymer* 1982, **23**, 000
- 5 Nomura, S., Kawai, H., Kimura, I. and Kagiya, M. *J. Polym. Sci. A-2* 1970, **8**, 383
- 6 Andersson, L. and Nordén, B. *Chem. Phys. Lett.* 1980, **75**, 398
- 7 Kimura, I., Kagiya, M., Nomura, S. and Kawai, H. *J. Polym. Sci. A-2* 1969, **7**, 709
- 8 Ward, I. M. 'Structure and Properties of Oriented Polymers', Applied Science Publishers, London, 1975, p. 32
- 9 Kratky, O. *Kolloid-Z.* 1933, **64**, 213
- 10 Hennecke, M. and Fuhrmann, J. *Colloid Polym. Sci.* 1980, **258**, 219
- 11 Chapoy, L. L., Spaseska, D., Rasmussen, K. and Duprés, D. B. *Macromolecules* 1979, **12**, 680

## Intrinsic viscosity of cellulose derivatives and the persistent cylinder model of Yamakawa

S. Dayan, P. Maissa, M. J. Vellutini and P. Sixou

Laboratoire de Physique de la Matière Condensée, C.N.R.S. L.A. 190, Université de Nice, Parc Valrose, 06034 Nice Cedex, France

(Received 28 July 1981; revised 14 January 1982)

By using the chain model proposed by Yamakawa, intrinsic viscosity measurements allow characterization of cellulose derivatives in dilute solution by persistence length and hydrodynamic diameter as a function of different parameters such as temperature of solvents, degree of substitution and type of substituent.

**Keywords** Intrinsic viscosity; polymer; solution; persistence length; cellulose derivatives

Anisotropic phases are formed in concentrated solutions of certain rigid polymers. The best known examples are the aromatic polyamides which have been studied with the help of various physico-chemical methods<sup>1-7</sup>. Recently, it has been demonstrated that polymer chains of lesser rigidity, such as the cellulose derivatives, can also form mesomorphic solutions at high concentrations, between 20 and 50 wt%<sup>8-13</sup>. The concentration at which the anisotropic phase appears depends not only on the type of solvent but also on characteristics of the chain such as degree of substitution, type of substituent and so on.

In these discussions a parameter of some importance is the chain rigidity. To gain an insight into the concentration dependence of the rigidity, we firstly studied dilute solutions and have investigated the intrinsic viscosity for a number of cellulose derivatives.

Over a sufficiently small range of polymer molecular mass the intrinsic viscosity  $[\eta]$  can be fitted to the

empirical Mark-Houwink equation<sup>14</sup>:

$$[\eta] = K.M^\alpha \quad (1)$$

where  $K$  and  $\alpha$  are constants for a given polymer-solvent system. Qualitatively,  $\alpha$  increases with increasing chain rigidity, but for a more complete analysis, it is necessary to consider a more detailed theoretical model such as that proposed by Yamakawa<sup>15</sup>. Some authors have used this model and graphical methods to estimate the persistence length of flexible chains<sup>16-18</sup> and of  $\alpha$ -helical polypeptides<sup>19</sup>. Following ideas first proposed by Arpin<sup>20</sup>, we have calculated the hydrodynamic diameter and the persistence length from experimental values of intrinsic viscosity and molecular mass for a large variety of polymer systems. By refining and extending the method of Arpin, we have been able to obtain a systematic analysis of cellulose derivatives in solution.